Platinum Nanofilm Formation by EC-ALE via Redox Replacement of UPD Copper: Studies Using in-Situ Scanning Tunneling Microscopy

Youn-Geun Kim, Jay Y. Kim, Deepa Vairavapandian, and John L. Stickney*
Department of Chemistry, University of Georgia, Athens, Georgia 30602
Received: June 16, 2006; In Final Form: July 24, 2006

The growth of Pt nanofilms on well-defined Au(111) electrode surfaces, using electrochemical atomic layer epitaxy (EC-ALE), is described here. EC-ALE is a deposition method based on surface-limited reactions. This report describes the first use of surface-limited redox replacement reactions (SLR^3) in an EC-ALE cycle to form atomically ordered metal nanofilms. The SLR^3 consisted of the underpotential deposition (UPD) of a copper atomic layer, subsequently replaced by Pt at open circuit, in a Pt cation solution. This SLR^3 was then used a cycle, repeated to grow thicker Pt films. Deposits were studied using a combination of electrochemistry (EC), in-situ scanning tunneling microscopy (STM) using an electrochemical flow cell, and ultrahigh vacuum (UHV) surface studies combined with electrochemistry (UHV-EC). A single redox replacement of upd Cu from a $PtCl_4^{2-}$ solution yielded an incomplete monolayer, though no preferential deposition was observed at step edges. Use of an iodine adlayer, as a surfactant, facilitated the growth of uniformed films. In-situ STM images revealed ordered Au(111)−$(\sqrt{3} \times \sqrt{3})R30°$-iodine structure, with areas partially distorted by Pt nanoislands. After the second application, an ordered Moiré pattern was observed with a spacing consistent with the lattice mismatch between a Pt monolayer and the Au(111) substrate. After application of three or more cycles, a new adlattice, a (3×3)-iodine structure, was observed, previously observed for I atoms adsorbed on Pt(111). In addition, five atom adsorbed Pt−I complexes randomly decorated the surface and showed some mobility. These pinwheels, planar PtI_4 complexes, and the ordered (3×3)-iodine layer all appeared stable during rinsing with blank solution, free of I^- and the Pt complex ($PtCl_4^{2-}$).

Introduction

Understanding and control in the electrochemical deposition of atomic and molecular layers is of fundamental importance to the electrochemical growth of nanofilms and of great technological significance. Fields such as nanostructure synthesis, electrocatalysis, magnetic materials, and the formation of ULSI (ultra large scale integrated circuits), all stand to benefit if electrochemical methods can be applied with atomic and molecular level control.

It is of particularly interest to study the atomic layer growth of nanofilms of noble metals by electrochemical deposition, given their extreme stability, conductivity, and importance in catalysis. Electrochemical methodologies are rightly seen as simple, versatile, and relatively low cost. If atomic level control can be added to the benefits of electrodeposition, direct competition with vacuum and gas-phase processes, such as molecular beam epitaxy (MBE) and chemical vapor deposition (CVD), will result.

In electrodeposition heteroepitaxial growth of an atomic layer of one metal on a second has been extensively performed and is generally referred to as underpotential deposition (UPD).[1] More recently, detailed studies of the structures formed during UPD on single-crystal surfaces have been performed with increasing frequency.[2−6] UPD is a phenomenon where an atomic layer of one metal deposits on a second, at a potential prior to that needed to electrodeposit the element on itself, the result of the free energy of formation of a surface compound or alloy. Examples of UPD include the deposition of less-noble metals such as copper,[7−10] silver,[11−13] or lead[14,15] onto gold electrodes, all known to form uniform epitaxial atomic layers. UPD, however, is by definition limited to an atomic layer. Au and Pt cannot be deposited at UPD, due to their slow electrodeposition kinetics. Atomic level studies of the epitaxial growth of successive atomic layers of noble metals are rare. Attempts to grow atomic layers tend to result in formation of clusters, rather than epitaxial deposits, the result of their high cohesive energy.[16]

A number of researchers have used well-defined gold substrates to study the electrodeposition of Pt, which generally produced platinum particles. Scanning tunneling microscopy (STM) has been used extensively to characterize the size and distribution of these nanoclusters.[17−19] Although it is not an ideal layer by layer process, Uosaki et al. have achieved quasi-two-dimensional layer by layer growth of Pt atoms on Au(111), by the electrochemical reduction of $PtCl_6^{2-}$ complexes.[17] Recently, Waibel et al. performed a similar study and showed that ordered adlayers of the $PtCl_4^{2-}$ complex can be formed and that nucleation of Pt started predominantly at defects, such as step edges. At low deposition rates, three-dimensional clusters were formed.[18] Nagahara et al. examined Pt nanoparticles produced from solutions of haloplatinate complexes, PtX_4^{2-} (X = Cl, Br, I), on Au(111). STM images showed well-ordered pinwheel features for the $PtCl_4^{2-}$ and $PtBr_4^{2-}$ solutions, though not with the PtI_4^2 complex. They were able to reduce these Pt complexes, forming particles with diameters of 3.0 and 0.46 nm in height.[19]

The electrodeposition of metal thin films, in general, is an important commercial process. On the other hand, it is well-known that depositions of Pt and Au frequently result in less than optimal deposits, due to the irreversibility of the processes. The studies described here involve the development of a layer by layer deposition methodology, via electrochemical atomic layer epitaxy (EC-ALE), where deposits are formed an atomic

* To whom correspondence should be addressed. E-mail: stickney@chem.uga.edu.

10.1021/jp063766f CCC: $33.50
Published on Web 08/22/2006

layer at a time using surface-limited reactions. EC-ALE is the electrochemical analogue of atomic layer epitaxy (ALE) and atomic layer deposition (ALD),[20−22] all methods based on the growth of materials an atomic layer at a time using surface limited reactions. This article describes the first instance of atomic layer characterization of the epitaxial growth of multiple atomic layers of a metal, facilitated by the use of EC-ALE.

EC-ALE was developed by combining the principles of ALE, specifically, the growth of materials an atomic layer at a time, with UPD, for the formation of compound semiconductors.[23−25] Compounds formed include many of the II−VIs, including Zn-, Cd-, and Hg-based chalcogenides, as well as some III−Vs, V−VIs, and IV−VI compounds. In the growth of compounds, the UPD of the elements making up a compound can be alternated to grow compound nanofilms. As noted above, UPD of a metal on itself cannot be performed, by definition, so the strict application of UPD in a simple cycle will not result in the growth of nanofilms of pure metal.

Recently, Adzic and Brankovic et al. illustrated that a predeposited, surface-limited, Cu UPD adlayer can be used as a sacrificial layer, to control the growth of a submonolayer amount of Pt on Au(111), by exchanging the Cu in a Pt ion solution at open circuit (OC). Their results suggested the growth of very small, monatomically high, nanoclusters randomly distributed over the surface.[26] Such reactions are referred to here as surface-limited redox replacement reactions (SLR^3). Despite the random distribution of these nanoparticles, the results of Brankovic et al. suggested it may be possible to form ideal single-crystalline nanofilms of Pt by repeating this SLR^3 in a layer by layer methodology: EC-ALE. In fact, Weaver et al. attempted to grow Pt nanofilms by repeated application of the SLR^3.[27]

This article describes studies of the atomic layer growth of Pt nanofilms, using this SLR^3 in an EC-ALE cycle. That is, Cu UPD layers were replaced by Pt, using a $PtCl_4^{2-}$ solution at open circuit, as outlined by Brankovic et al.[26] The spontaneous process was driven by the difference in formal potentials between Pt metal and UPD Cu, the difference in free energies. The standard potential for Pt ($PtCl_4^{2-}$/Pt), 0.52 V (vs Ag/AgCl),[28] is well positive of the formal potential for Cu^{2+}/Cu_{upd}, ~0.2−0.25 V, on gold.

The depositions were followed using an EC−STM flow cell on Au(111). The electrochemical flow cell for the in-situ STM studies was developed by this group and allowed solution exchange while maintaining potential control and while imaging. This cell was developed for studied of the electrodeposition of compound semiconductor nanofilms, an atomic layer at a time using EC-ALE.[29]

This paper describes the deposition process in the presence of an adsorbed layer of I atoms, used as a surfactant. I atoms are known to protect some metal surface, such as Pt, from contamination. Adsorbed halides in general are known to facilitate surface diffusion in electrolyte solutions and thus promote "electrochemical annealing."[30] In addition, the corrugations of halide atomic layers are strong in STM studies, making imaging of such surface somewhat easier.[31] Finally, it is well-known that electrodeposition of Cu and Ag on Pt or Au surfaces coated with an I atom layer occurs, with the depositing metal inserting between the I atom layer and the metal substrate, suggesting that the I atoms float on the depositing metal surface.[2,3] Figure 1 is a cartoon of a SLR^3 starting with an I atom layer for the formation of ideal Pt nanofilms.

Experimental Section

For the in situ scanning tunneling microscopy experiments (EC-STM), Au single-crystal surfaces were prepared using a

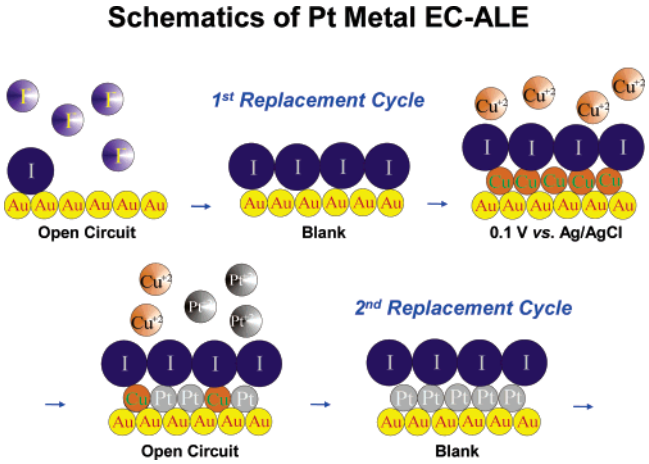

Figure 1. Schematics of an EC-ALE cycle for the formation of Pt nanofilms on iodine-modified Au(111) electrode.

variation of the Clavilier method.[32,33] The flame-annealed bead electrode was quenched in Milli-Q Plus (Millipore, Houston, TX) water of a resistivity >18.2 MΩ, previously deaerated with hydrogen gas. This bead was then quickly transferred through air, with a protective water film, into the EC-STM cell.

The EC-STM flow cell used for in-situ STM studies allowed flow and exchange of solutions over the Au bead working electrode. The reference/auxiliary compartment was downstream, to avoid contamination. Low flow rates in and out of the cell were equivalent, to maintain the solution level in the cell, using a single peristaltic pump, flow rate = 0.9 mL/min, as described previously.[29] In both the EC-STM and voltammetric measurements, the supporting electrolyte consisted of 0.1 M $HClO_4$ or 0.05 M H_2SO_4 prepared from doubly distilled $HClO_4$ and H_2SO_4 (Aldrich Chemicals, Milwaukee, WI) and Milli-Q Plus water. Ultrapure-grade K_2PtCl_4, H_2PtCl_6, and $CuSO_4$ (Aldrich Chemicals, Milwaukee, WI) were used. The three-electrode electrochemical cell included an Au-wire auxiliary electrode and a 3 M Ag/AgCl reference electrode (BAS); unless otherwise specified, all potentials are reported with respect to this reference electrode. EC-STM experiments were performed with a Nanoscope III (Digital Instruments, Santa Barbara, CA), equipped with W tips, electrochemically etched (15 VAC in 1 M KOH) from a 0.25 mm wire. The tip was coated with transparent nail polish to minimize Faradaic currents. Prior to each experiment, the presence of a well-ordered Au(111)-(1 × 1) structure in pure supporting electrolyte was verified by wide-angle and atom-resolved EC-STM scans, prior to injection of 1 mM Cu^{2+} or 0.1 mM $PtCl_4^{2-}$ solutions into the EC-STM flow cell.

Low-energy electron diffraction (LEED; Princeton Research Instruments) and Auger electron spectroscopy (AES; Perkin-Elmer, Eden-Prairie, MN) were performed in an ultrahigh vacuum system which allowed sequential electrochemical and surface analytical measurements, without exposure of the sample to air. This process of using UHV surface analytical techniques in studies of electrode surfaces is referred to as UHV-EC methods.[34] The electrode used for the UHV-EC studies was the Au(111) single crystal slice, 99.999 % pure, commercially oriented and polished from MaTecK, GmbH. The crystal was cleaned with multiple cycles of Ar^+-ion bombardment and annealing prior to each experiment. LEED and AES were used to check surface composition and structure, prior to each experiment. Voltammetric studies were performed using this 1 cm diameter Au(111) single-crystal slice, 0.1 cm thick. The polycrystalline sides contributed to the voltammetry, as well as the (111) faces, as the whole crystal was immersed.

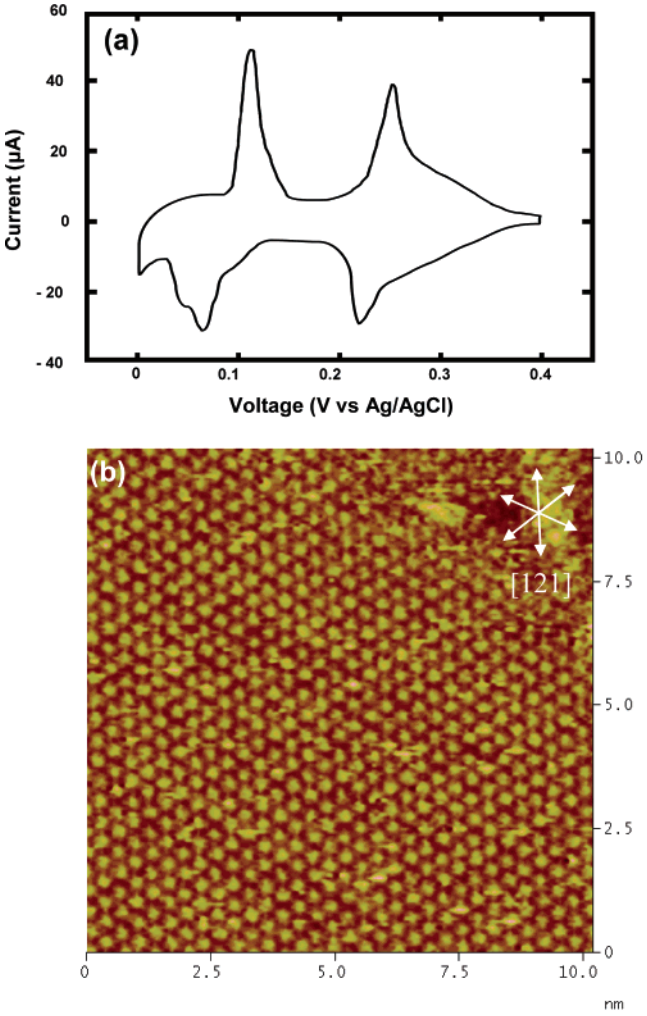

Figure 2. (a) Steady-state cyclic voltammogram for Cu UPD on Au(111) in 0.05 M H_2SO_4 and 1 mM $CuSO_4$ solution. Potential sweep rate: 5 mV/s. (b) EC-STM image of the honeycomb ($\sqrt{3} \times \sqrt{3}$)*R*30° structure obtained at +0.15 V. Bias voltage: −150 mV. Tunneling current: 20 nA.

Results and Discussion

The cyclic voltammogram for Cu UPD on Au(111) in a 0.05 M H_2SO_4 and 1 mM $CuSO_4$ solution (Figure 2a) was very similar to those reported for studies of gold single-crystal electrodes previously reported.[9,11] The two peaks at +0.23 and +0.05 V correspond to formation of two distinctly different ordered Cu UPD adlayers. Cu coverages of 2/3 and 1/3 monolayer (ML), respectively, were deposited in the first and second deposition peaks, respectively. A ML is defined in this paper as one adsorbate for every Au surface atom. At +0.15 V, the first Cu UPD peak resulted in the honeycomb ($\sqrt{3} \times \sqrt{3}$)*R*30° structure at a Cu coverage of 0.67 monolayer (ML), while, after the second peak, the remaining 0.33 ML of Cu was deposited at 0.0 V, completing a full Cu ML. In the first UPD structure, (bi)sulfate anions occupied the centers of Cu hexagons, the honeycomb structure, with an anion coverage of 1/3 ML, known from the literature.[35−38] This structure (Figure 2b) remained stable during rinsing with blank at controlled potential in the STM flow cell. A 0.1 mM $PtCl_4^{2-}$ + 0.1 M $HClO_4$ solution was introduced at open circuit (OC) to replace the Cu UPD layer. During solution exchange, the OC potential shifted to 0.6 V, over the course of 3 min, a potential positive enough to suggest that all Cu had been replaced, subsequently confirmed via Auger. The cell was then rinsed with blank.

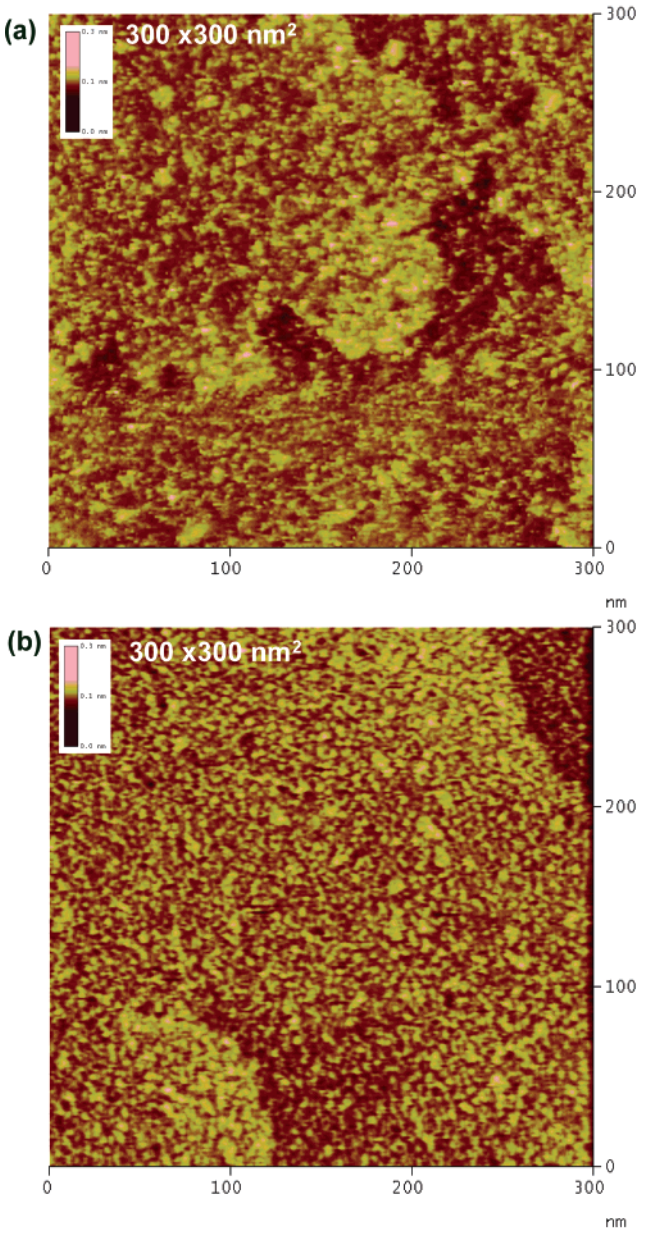

Figure 3. (a) Wide-area EC-STM images of the Pt submonolayer on Au(111) obtained by replacement of Cu UPD layer in 0.1 M $HClO_4$ solution at OC potential. (b) After I covered Pt submonolayer. Bias voltage: −350 mV. Tunneling current: 20 nA.

During the redox replacement, imaging continued in the EC-STM flow cell, allowing observation of large scale morphology changes. Figure 3a is a representative STM image of the surface after the SLR[3], a relatively uniform distribution of Pt clusters over the entire 300 × 300 nm surface, imaged at OC. The image suggests a continuous layer was not formed nor were large islands, nothing that suggests a two-dimension epitaxial deposit. These results show no evidence that the SLR[3] resulted in direct electron transfer from one Cu atom to a Pt ion, direct adatom−ion interaction, or in surface mediated transfer which should allow Pt deposition anywhere on the surface, regardless of the Cu atom site. Pt ions appear to reduce to Pt adatoms and then diffuse over the surface, creating very small Pt adatom clusters.

The stoichiometry of the SLR[3] limits Pt deposition to at most a submonolayer (2/3 ML) on Au(111). It is entirely possible that even less Pt was actually deposited, raising the question of redox replacement efficiency. Determination of the efficiency was one of the challenges of this work, how to quantify the Pt deposited. Electrochemical stripping characterization via Pt

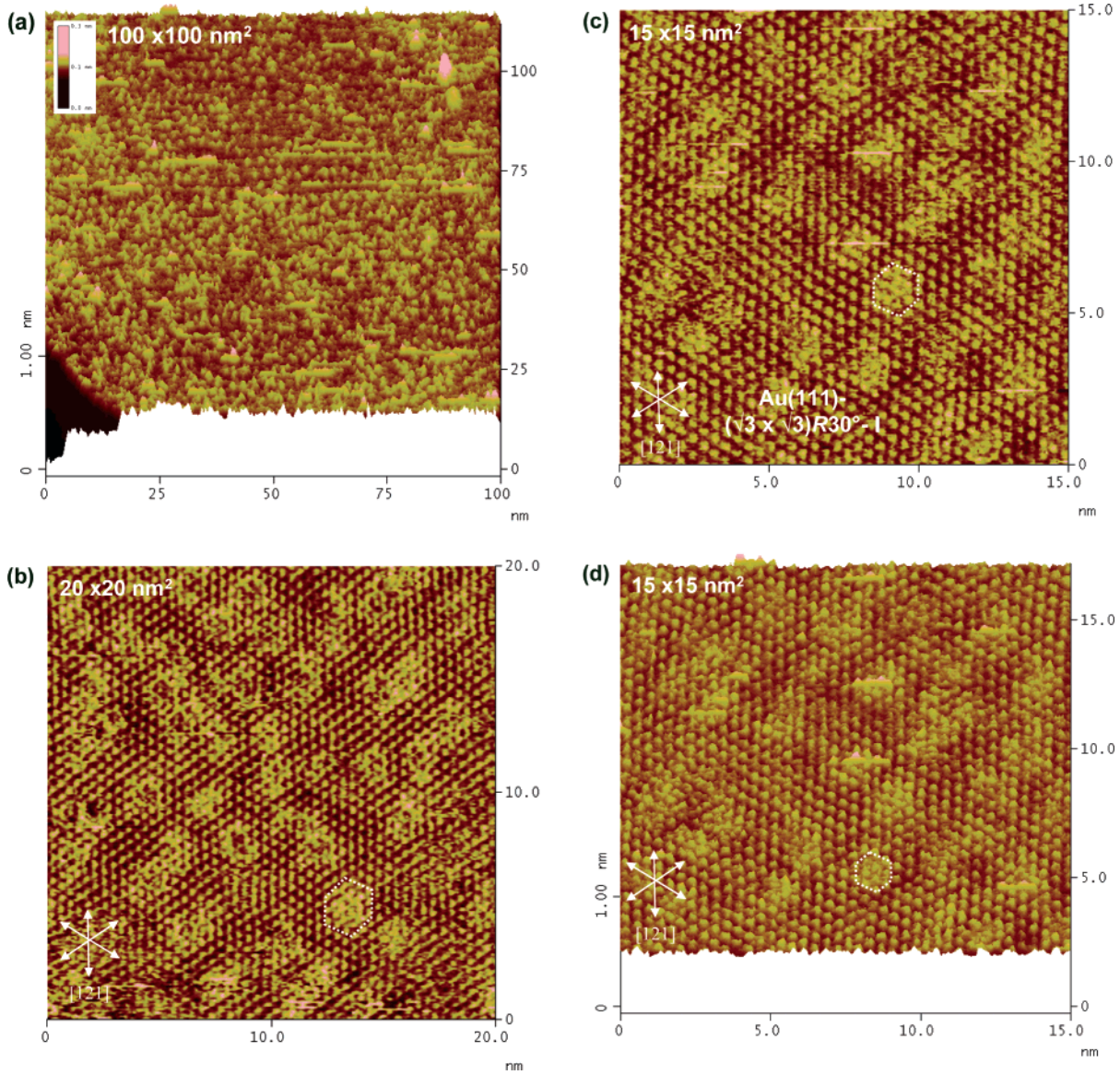

Figure 4. Height-shaded plot images of the Pt submonolayer on Au(111) in 0.1 M $HClO_4$ solution at OC potential: (a) 100 nm × 100 nm; (d) 15 nm × 15 nm. High-resolution EC-STM images showing the $(\sqrt{3} \times \sqrt{3})R30°$-I adlayer consists of hexagonal arrays: (b) 20 nm × 20 nm; (c) 15 nm × 15 nm. Bias voltage: −250 mV. Tunneling current: 20 nA.

coulometry was not possible. In addition, Auger spectra for Au and Pt are so similar that independent quantification of Pt and Au was not possible. XPS should allow characterization of submonolayer amounts of Pt, even in the presences of Au, and is presently being upgraded on the UHV-EC instrument.

It is well-known that various electrochemical processes, such as hydrogen and metal UPD, are strongly affected by coadsorbed electrolyte.[3,34,39] In particular, adsorbed iodine enhancing surface mobility on single-crystal surfaces has been studied in detail with Cu, Au, and Pd single-crystal electrodes using UHV-EC and EC-STM techniques.[30,40,41] For example, disordered Pd(111) surfaces can be spontaneously reordered upon exposure, at ambient conditions, to a dilute aqueous solution of iodide.[41] This process is, in part, responsible for "electrochemical annealing", which can also be promoted by the use of relatively positive potentials, where the exchange current is maximized. In these studies, iodine adsorbate-induced surface ordering has been applied to facilitate the growth of more uniformed epitaxial Pt layers.

Figure 3b shows an STM image obtained for an iodine-covered Pt submonolayer after the first SLR^3 cycle (Figure 3a). This 300 nm × 300 nm STM image shows a more uniform distribution of small nanoparticles, more two-dimensional, than for Pt deposits without the I atom layer. There is no sign of preferentially deposition along the step edges, a frequent site for three-dimensional growths in conventional electrodeposition. Extended terraces are clearly visible in Figure 3b. Furthermore, a higher resolution view (100 nm × 100 nm) of the terrace (Figure 4a) reveals a uniform distribution of 1−3 nm wide and 0.1 nm high particles over the entire area (Figure 4a). A closer view (Figure 4b) reveals the particles' distorted hexagonal shapes. These features display a corrugation of only 0.08 nm. It must be noted that these images are actually of the I atoms adsorbed on the Pt particles and the Au(111) surface. From a vast number of halide adsorption studies on metal surfaces it is known halides tend to form close-packed hexagonal adlayers, with excellent surface mobility. In general, a halide atom will form one bond, and thus they do not tend to bond to each other and are present at near their van der Waals diameters (0.5 nm). At higher potentials, I atoms are bonded to each other, resulting in the formation of I_2 molecules which diffuse away. The point is, I atom layers acts as a blanket over the surface, covering and conforming to the underlying surface features.

The ordered hexagonal iodine adlayer has close-packed iodine atomic rows, rotated 30° from the atomic rows in the Au(111).

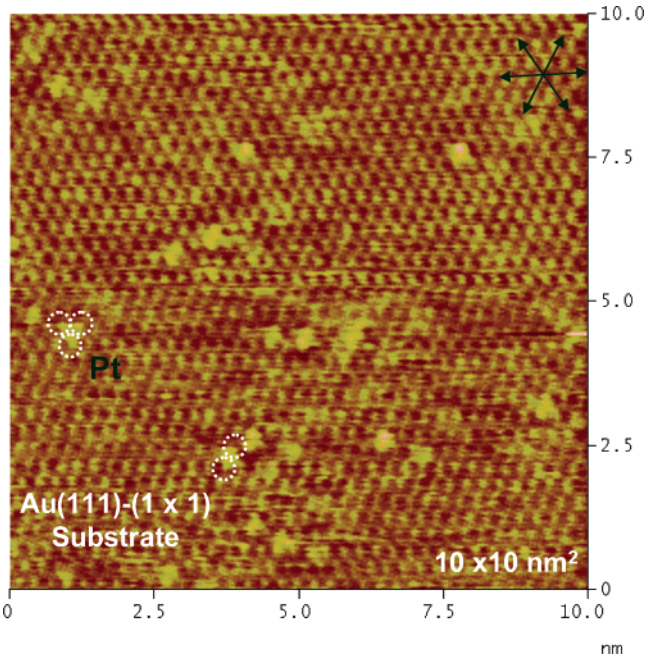

Figure 5. High-resolution EC-STM image showing the isolated Pt atoms as well as Pt dimers and trimers, with in the close-packed Au-(111)-(1 × 1) substrate surface in 0.1 M $HClO_4$ solution obtained when the tunneling current was abruptly changed from 20 to 50 nA during the scan. Bias voltage: −150 mV. Tunneling current: 50 nA.

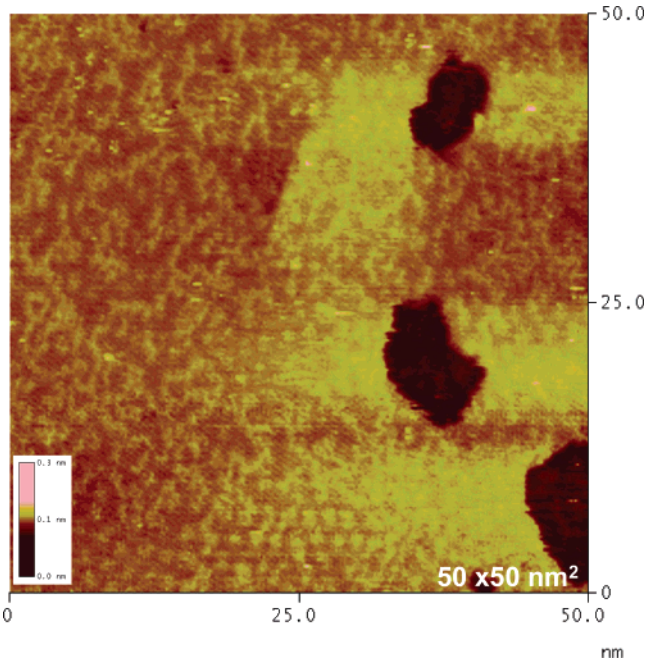

Figure 6. Wide-area EC-STM images of the Pt layer after second Pt metal EC-ALE cycle in 0.1 M $HClO_4$ solution at OC potential. Bias voltage: −340 mV. Tunneling current: 25 nA.

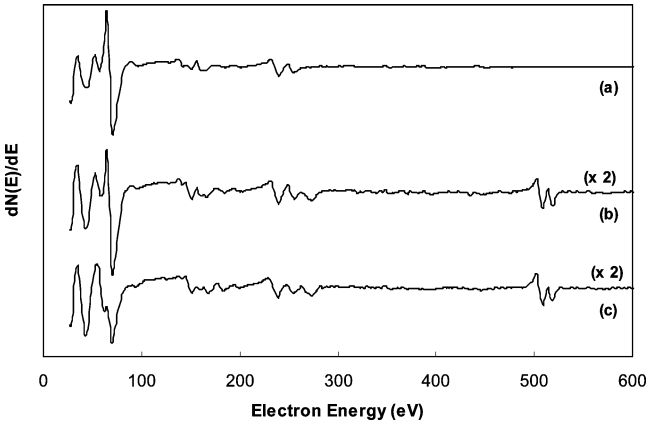

Figure 7. Auger electron spectrums of (a) clean Au(111), (b) after two cycles of Pt replacements, and (c) after four cycles of Pt replacements.

Arrows drawn in Figure 4c,d denote the directions of the $\sqrt{3}$ unit vectors ([121]), characterizing this structure as a Au(111)−($\sqrt{3} \times \sqrt{3}$)*R*30°-I.[42] The surface appears to be a similar hexagonal array of I atoms but with a series of hexagonally shaped clusters, varying between 1.0 and 3.5 nm, and presumably associated with the deposited Pt atoms. The hexagonal features suggest significant order to the deposited Pt atoms.

To learn more about these features and the nucleation of Pt on the I-coated Au(111) surface, EC-STM experiments were performed using increased tunneling currents, to try and image the underlying Pt particles. Figure 5 is a "dynamic tunneling current" STM image, where the tunneling current was abruptly changed from 20 to 50 nA, at OC, revealing a surface decorated with isolated Pt atoms as well as Pt dimers and trimers. These atoms appear to exist within the close-packed Au(111)-(1 × 1) substrate surface structure. Note in Figure 4a the monatomic step edge, in the lower left corner, which shows the corrugation due to the Pt clusters is much less than an atom in height, only about 0.08 nm. This strongly suggests that the first partial monolayer of Pt atoms deposited with the SLR[3] are not present as adatoms but incorporated into the Au(111) surface to form a surface alloy. Some Pt atoms may go subsurface as well. The image also shows that the Pt atoms are almost perfectly incorporated into the parallel atomic rows of the Au(111) surface.

The first assumption would be that the Pt atoms are present in hexagonal islands, or rings, from images of the I atom layer (Figure 4). However, given the apparent distribution of, and presence in the surface of, the Pt atoms (Figure 5), it is more likely that the dispersed Pt atoms, dimmers, and trimers only cause a limited perturbation in the overlying I layer. This disturbs the ($\sqrt{3} \times \sqrt{3}$)*R*30°-I hexagonal array structure and produces hexagonal rings of I atoms pushed from their ideal, low, 3-fold sites, accounting for the observed images (Figure 4).

In this study, after one SLR[3] cycle, it appears the Pt atoms incorporate into the Au layer, rather than on top, while, without the I atom layer, the Pt nanoclusters appear on top.[43] The Pt atom incorporation appears random, not preferentially near or at step edges, and shows little tendency to segregate forming larger, pure, Pt islands. Theoretically, the Pt coverage should be 0.66 ML, given one for one exchange of Cu for $PtCl_4^{2-}$. Such a high coverage is not consistent with the image shown in Figure 5, where high tunneling currents were used. It is probable that the exchange was not 100% efficient, and studies are underway to better quantify the exchange process.

The deposition began with exposure of the clean annealed Au(111) surface to the KI solution and formation of the ($\sqrt{3} \times \sqrt{3}$)*R*30°-I adlattice. The solution was then exchanged for blank, to flush I^- ions from the cell, and followed by introduction of the Cu^{2+} ion solution at +0.1 V, where it was held for 15 s or more. After Cu UPD, the deposit went OC while the $PtCl_4^{2-}$ solution was introduced, flushing Cu^{2+} ions from the cell and allowing exchange of the Cu UPD layer for Pt. Finally, the cell was rinsed again with the blank solution to remove excess $PtCl_4^{2-}$ ions. Given that I atoms strongly adsorb to Pt, Cu, and Au, significant loss of I atoms during a cycle was not expected. However, an extra step, exposure of the surface to a 0.1 mM KI solution, could be added to renew the I atom layer. Alternatively, the cycle can simply begin again with Cu UPD at +0.1 V.

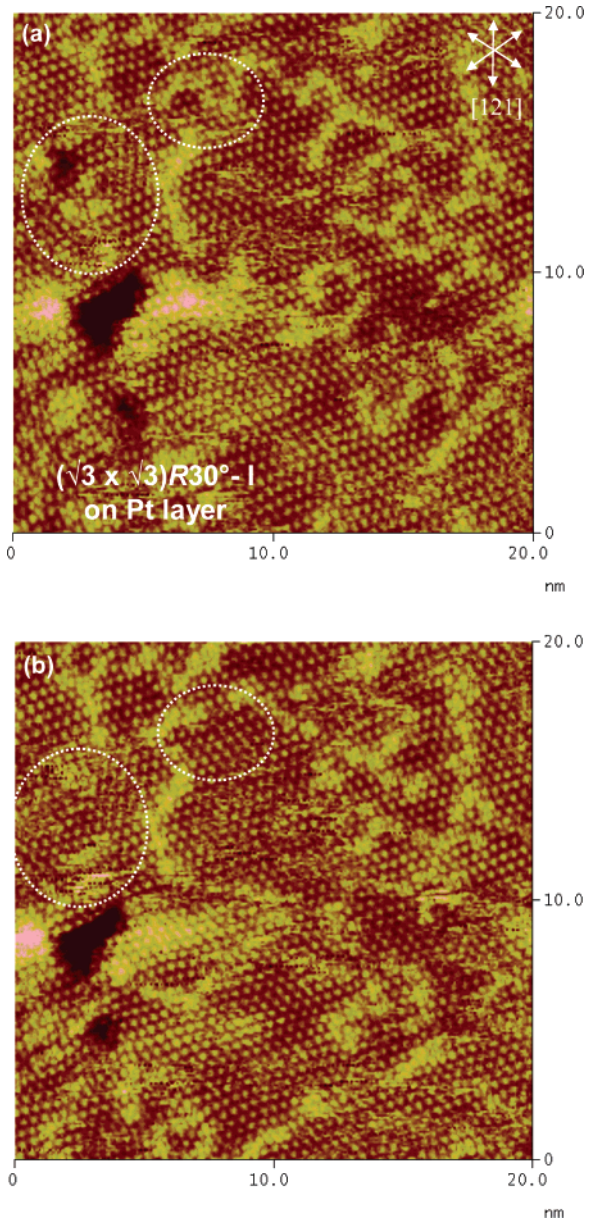

Figure 8. High-resolution EC-STM images of the Pt layer after second Pt metal EC-ALE cycle. Two images, taken 1 min apart, show the arrangements of adlayers consisting of five atom clusters and I in 0.1 M $HClO_4$ solution at OC potential. Bias voltage: −250 mV. Tunneling current: 20 nA.

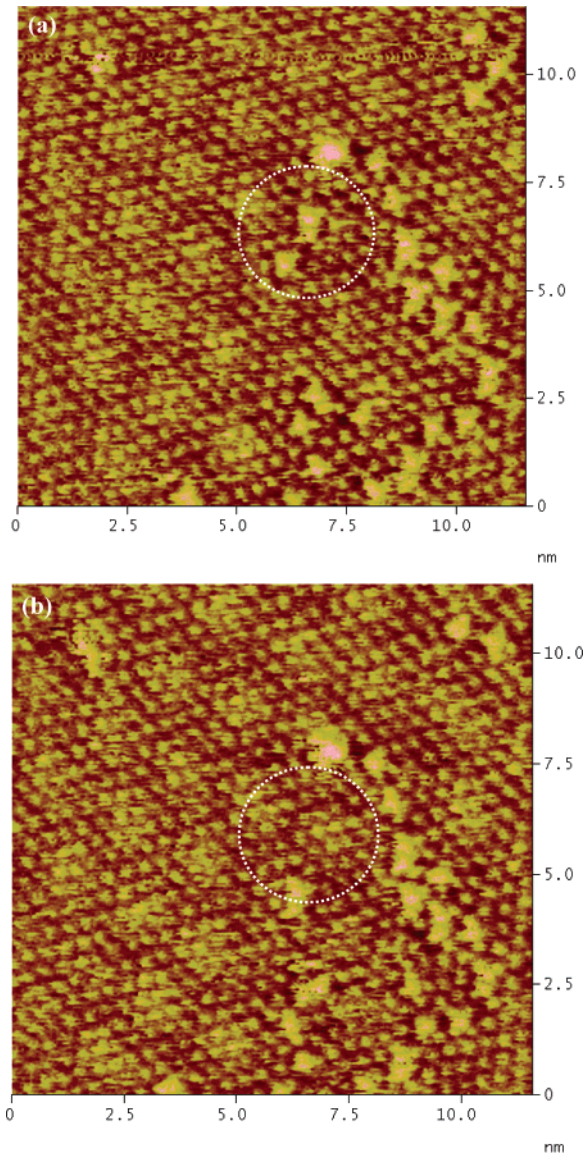

Figure 9. High-resolution EC-STM images showing the formation of a Moiré pattern on the Au(111) surface after second Pt metal EC-ALE cycle. Two images, taken 1 min apart, show the formation of a Moiré pattern on the surface consisting of five atom clusters and I in 0.1 M $HClO_4$ solution at OC potential. Bias voltage: −300 mV. Tunneling current: 25 nA.

Figure 6 was taken after a second SLR[3], equivalent to that shown in Figure 1. Instead of the hexagons (Figure 4) observed after one cycle, the bright features on this surface appear more like chains on a hexagonal background of I atoms. Figure 7 displays Auger spectra taken after two and four SLR[3] of Cu replacement by Pt. Although the Pt signals are not differentiable from those for Au, the presence of the I atom layer is clearly evident by the doublet at 500 eV. Closer inspection (Figure 8) suggests the chains were composed of five atom clusters (discussed below). The two images in Figure 8 were taken 1 min apart, indicating that some clusters have moved and some have remained stationary while others have disappeared. There are indications that some of the clusters are disappearing, while pits in the surface are filling. Figure 9 shows the formation of a Moiré pattern on the surface, suggesting that the Pt layer has been completed, and involves a lattice mismatch between the Pt and Au. As noted, the I atoms act as a cover, indicating that the Moiré pattern results from the lattice mismatch between the Au(111) substrate and a monolayer of Pt atoms. Figure 10 presents a structure proposed to account for Figure 9. The proposed structure shows a $(\sqrt{37} \times \sqrt{37})R25.29°$ match between the Au(111) surface and a Pt(111) monolayer, with the I atoms adopting a $(\sqrt{3} \times \sqrt{3})R30°$ arrangement with respect to the Pt monolayer. The period and rotation of the Moiré pattern are consistent with the lattice mismatch between metallic Au (2.88 nm) and Pt (2.78 nm).

Figure 11 shows an image of the surface after a third SLR[3] deposition cycle, displaying a new I atom structure, a (3×3)-I, previously observed on Pt(111) surfaces.[31,44,45] This is a strong indication that a Pt atomic layer has been formed. Also evident in Figure 11 is a significant disorder and an increased coverage of the five atom clusters.

That some islands were formed on the surface after three SLR[3] cycles is consistent with the fact that the coverage of Cu deposited each cycle is less than a monolayer. Studies of Cu UPD on I-coated Au have suggested a coverage of only ~0.44 ML, forming a (3×3) structure,[46] while Cu deposition on Pt-

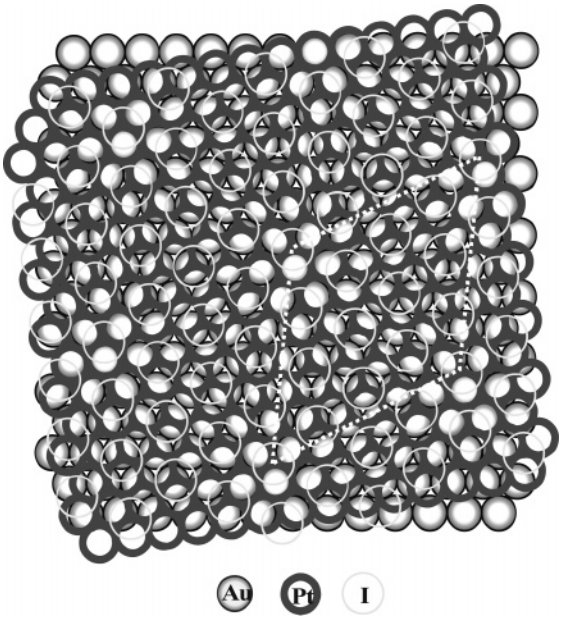

Figure 10. Structure proposed to account for the Moiré pattern observed in Figure 9. The structure shows a $(\sqrt{37} \times \sqrt{37})R25.29°$ match between the Au(111) surface and a Pt(111) monolayer, with the I atoms adopting a $(\sqrt{3} \times \sqrt{3})R30°$ with respect to the Pt monolayer. The period and rotation of the Moire pattern are consistent with the lattice mismatch between metallic Au (2.88 nm) and Pt (2.78 nm).

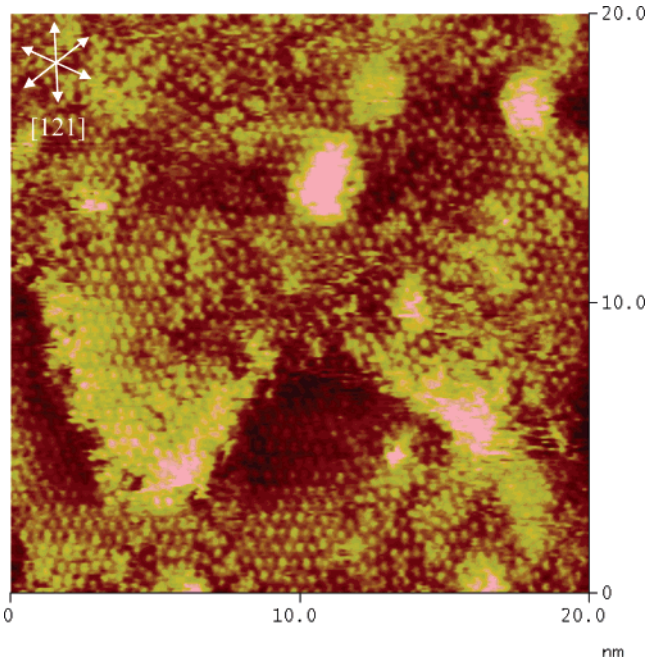

Figure 11. High-resolution EC-STM image of the Pt layer after a third Pt metal EC-ALE cycle. This image shows a new I atom structure developing on the surface, a (3 × 3)-I on deposited Pt layer. Bias voltage: −250 mV. Tunneling current: 20 nA.

(111) surface coated with I atoms results in a coverage of 0.44 ML, as well.[3] Thus after two cycles, a little under a ML would be expected if the conversion efficiency was 100%. The relative homogeneity and the presence of a moiré pattern after two cycles suggest that a near full monolayer was formed after two cycles. This would then suggest that the coverage after three cycles would be closer to 1.5 ML, rather than two, and would explain the presences of some island like features on the surface.

Figure 12 shows a high-resolution image of the five atom clusters. Similar features have been seen in a number of studies of PtX_4^{2-} (X = Cl, Br, I).[18,19] It is proposed here that these are

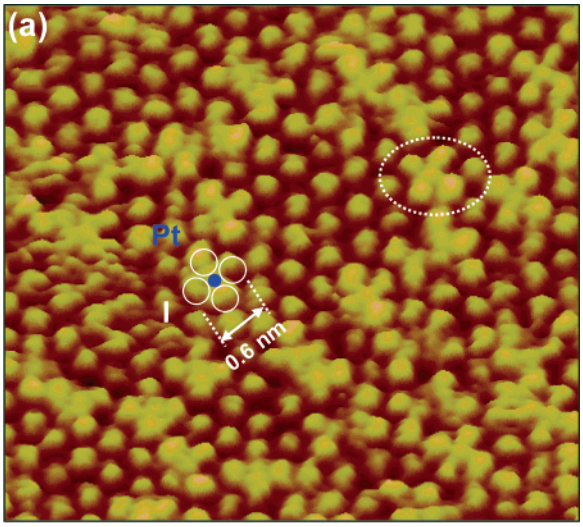

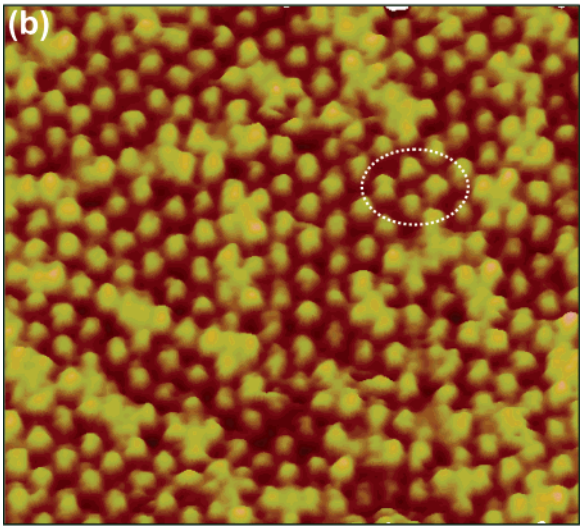

Figure 12. High-resolution image of the internal features of five atom clusters proposed to be one central discharged Pt atom in the center of four of the surface I atoms. Two images, taken 1 min apart, show the discharged Pt atom is commensurate with filling in underlying Pt atomic layer. Bias voltage: −300 mV. Tunneling current: 30 nA.

simply Pt adatoms that have not incorporated into a second layer of Pt yet. Some island like features appears to be composed of groups of these clusters. It is proposed here that the clusters are composed of a discharged Pt atom in the center of four surface I atoms. Again, repetitive scans show that these Pt atoms have mobility on the surface, facilitating electrochemical annealing.[47] Real time EC-STM images clearly shows that the number of 5 atom clusters goes down with time, as they diffuse, forming second layer Pt islands or domains.

Some care must be taken when comparing previous EC-ALE works where UPD was used to deposit each atomic layer of the elements composing a compound, with the present use of a SLR[3]. UPD is a thermodynamic process, producing homogeneous equilibrium atomic layers. In a SLR[3] the process starts with UPD, but the atomic layer is then exchanged for a more noble atomic layer at OC. From these studies, well-ordered atomic layers result, using the I atom layer as a surfactant to promote annealing.

The alternated UPD of two elements to form a compound using EC-ALE does have an advantage, in that the chemistry

of forming a compound promotes deposition of a UPD layer of one element only where an atomic layer of the other exists, mandating layer by layer growth. In the present case, no such driving force exists; deposition of an atomic layer can deposit anywhere on the surface where the sacrificial metal exists, including on islands of Pt already formed. This does not suggest that the surface will roughen dramatically, only that it may show more tendency to roughen than a strictly layer by layer process. Atomic resolution imaging during growth will be required better understand any tendency.

If the exchange of Pt for Cu were direct, the electrons of one Cu atom transferring to one Pt ion, then layer by layer deposition should be promoted. However, if the surface mediates electron transfer, more roughening would be expected. Recent studies of an SLR[3] where Pb UPD was replaced by Cu have shown that if Pb UPD was performed on half the electrode, followed by exposure of the whole electrode to a Cu ion solution, from Auger, Cu was observed to only deposit where the Pb UPD was present, suggesting that direct transfer may be occurring. If electrode-mediated electron transfer was predominant, Cu would be expected to deposit on areas devoid of Pb UPD, as well.

Conclusion

This paper represents the first atomic level study of the repeated application of an SLR[3] in an EC-ALE. Use of an I atom atomic layer as a surfactant served to promote layer by layer growth and the formation of well-ordered deposits. It appears that the first atomic layer of Pt deposited resulted in a surface alloy, while deposition of a second Pt atomic layer resulted in formation of a well-ordered Pt adlayer, producing a Moiré pattern in the I atom layer. The Moiré pattern is easily explained by the lattice mismatch between Pt and Au. The pattern appears to correspond to a $(\sqrt{37} \times \sqrt{37})R25.29°$ unit cell between the Au and Pt and a $(\sqrt{3} \times \sqrt{3})R30°$ between the Pt and I atoms.

Along with formation of the Moiré pattern, evidence of five atom clusters was seen distributed across the surface. Those clusters appear mobile and disappear with time, commensurate with filling in pits in the surface. It is proposed that the clusters are neutral Pt atoms surrounded by four I atoms. When the cluster finds a site, the Pt atom inserts, filling pits in the surface.

After a third SLR[3], the I atom layer changed from a $(\sqrt{3} \times \sqrt{3})R30°$-I, generally observed on Au(111), to a (3×3)-I structure, observed on Pt. Thus, there appears to be a transition from the Au to the Pt that starts with simply alloying the Pt into the Au(111) surface (first cycle), followed by formation of a full Pt atomic layer, where a lattice mismatch results in a Moiré pattern (second cycle). The Pt monolayer producing the Moiré pattern still supports a $(\sqrt{3} \times \sqrt{3})R30°$-I adlattice. However, after the third cycle, initiation of a second monolayer of Pt resulted and the Moiré pattern was gone, as was the $(\sqrt{3} \times \sqrt{3})R30°$-I structure. Apparently, the second Pt atomic layer supports a structure more similar to bulk Pt(111) than to Au-(111).

Electrochemical annealing is promoted by the presence of the I atom layer. Some mobility was evident in the five atom clusters, where the central atom was a zerovalent Pt, surrounded by four I atoms. Those clusters appear to diffuse across the surface, until the Pt atom is inserted into the growing Pt atomic layer. Alternatively, it may only be the Pt atom that diffuses, from 4-fold site in the I atom layer to the next I atom site.

Acknowledgment. Support from the National Science Foundation, Divisions of Materials and Chemistry, is gratefully acknowledged, as well as the Department of Energy (NNSA) under award No. DE-FG36-05GO85012.A000.

References and Notes

(1) Kolb, D. M. *Advances in Electrochemistry and Electrochemical Engineering*; Gerischer, H., Tobias, C. W., Eds.; John Wiley: New York, 1978; Vol. 11, p 125.
(2) Stickney, J. L.; Rosasco, S. D.; Song, D.; Soriaga, M. P.; Hubbard, A. T. *Surf. Sci.* **1983**, 130, 326−347.
(3) Stickney, J. L.; Rosasco, S. D.; Hubbard, A. T. *J. Electrochem. Soc.* **1983**, 131, 260−267.
(4) Aldaz, A.; Clavilier, J.; Feliu, J. M. *J. Phys. IV* **1994**, *4*, 75−93.
(5) Gewirth, A. A.; Niece, B. K. *Chem. Rev.* **1997**, *97*, 1129−1162.
(6) Herrero, E.; Buller, L. J.; Abruna, H. D. *Chem. Rev.* **2001**, *101*, 1897−1930.
(7) Magnussen, O. M.; Hotlos, J.; Nichols, R. J.; Kolb, D. M.; Behm, R. J. *Phys. Rev. Lett.* **1990**, *64*, 2929−2932.
(8) Magnussen, O. M.; Hotlos, J.; Beitel, G.; Kolb, D. M.; Behm, R. J. *J. Vac. Sci. Technol., B* **1991**, *9*, 969−975.
(9) Manne, S.; Hansma, P. K.; Massie, J.; Elings, V. B.; Gewirth, A. A. *Science* **1991**, *251*, 183−186.
(10) Hachya, T.; Honbo H.; Itaya, K. *J. Electroanal. Chem.* **1991**, *315*, 275−291.
(11) Kimizuka, N.; Itaya, K. *Faraday Discuss.* **1992**, *94*, 117−126.
(12) Corcoran, S. G.; Chakarova, G. S.; Sieradzki, K. *Phys. Rev. Lett.* **1993**, *71*, 1585−1588.
(13) Ogaki, K.; Itaya, K. *Electrochimi. Acta* **1995**, *40*, 1249−1257.
(14) Tao, N. J.; Pan, J.; Li, Y.; Oden, P. I.; DeRosa, J. A.; Lindsay, S. M. *Surf. Sci.* **1992**, *271*, L338-L344.
(15) Hsieh, S. J.; Gewirth, A. A. *Surf. Sci.* **2002**, *498*, 147−160.
(16) Bauer, E.; van der Merwe, J. H. *Phys. Rev. B* **1986**, *33*, 3657−3671.
(17) Uosaki, K.; Ye, S.; Naohara, H.; Oda, Y.; Haba, T.; Kondo, T. *J. Phys. Chem. B* **1997**, *101*, 7566−7572.
(18) Waibel, H. F.; Kleinert, M.; Kibler, L. A.; Kolb, D. M. *Electrochim. Acta* **2002**, *47* (9), 1461−1467.
(19) Nagahara, Y. H., M.; Yoshimoto, S.; Inukai, J.; Yau, S.-L.; Itaya, K. *J. Phys. Chem. B* **2004**, *108*, 3224−3230.
(20) Goodman, C. H. L.; Pessa, M. V. *J. Appl. Phys.* **1986**, *60*, R65−R82.
(21) Kuech, T. F.; Dapkus, P. D.; Aoyagi, Y. *Atomic Layer Growth and Processing*; Materials Research Society: Pittsburgh, PA, 1991; Vol. 222, p 360.
(22) Bedair, S. *Atomic Layer Epitaxy*; Elsevier: Amsterdam, 1993; p 304.
(23) Gregory, B. W.; Suggs, D. W.; Stickney, J. L. *J. Electrochem. Soc.* **1991**, *138*, 1279−1284.
(24) Stickney, J. L. *Electroanal. Chem.* **1999**, *21*, 75−209.
(25) Stickney, J. L. In *Advances in Electrochemical Science and Engineering*; Alkire, R. C., Kolb, D. M., Eds.; Wiley-VCH: Weinheim, Germany, 2001; Vol. 7, pp 1−105.
(26) Brankovic, S. R.; Wang, J. X.; Adzic, R. R. *Surf. Sci.* **2001**, *474*, L173−L179.
(27) Mrozek, M. F.; Xie, Y.; Weaver, M. J. *Anal. Chem.* **2001**, *73*, 5953−5960.
(28) Colum, F. *Standard Potentials in Aquous Solution*; Bard, A. J., Parsons, R., Jordan, J., Eds.; Marcel Dekker: New York, 1985; Chapter 16.
(29) Lay, M. D.; Sorenson, T. A.; Stickney, J. L. *J. Phys. Chem. B* **2003**, *107*, 10598−10602.
(30) Villegas, I.; Ehlers, C. B.; Stickney, J. L. *J. Electrochem. Soc.* **1990**, *137*, 3143−3148.
(31) Schardt, B. C.; Yau, S. L.; Rinaldi, F. *Science* **1989**, *243*, 1050−1053.
(32) Clavilier, J.; Faure, R.; Guinet, G.; Durand, R. *J. Electroanal. Chem. Interfacial Electrochem.* **1980**, *107*, 205−209.
(33) Soriaga, M. P.; Kim, Y.-G.; Soto, J. E. *Interfacial Electrochemistry*; Wieckowski, A., Ed.; Marcel Dekker: New York, 1999; p 249.
(34) Soriaga, M. P.; Stickney, J. L. *Modern Techniques in Electroanalysis*; Vanysek, Ed.; John Wiley & Sons: New York, 1996; Vol. 139, pp 1−58.
(35) Zei, M. S. Q., G.; Lehmpfuhl, G.; Kolb, D. M. *Ber. Bunsen-Ges. Phys. Chem.* **1987**, *91*, 349.
(36) Shi, Z. L. J. *J. Electroanal. Chem.* **1994**, *364*, 289−294.
(37) Shi, Z.; Lipkowski, J. *J. Electroanal. Chem.* **1994**, *365*, 303−309.
(38) Toney, M. F.; Howard, J. N.; Richer, J.; Borges, G. L.; Gordon, J. G.; Melroy, O. R. *Phys. Rev. Lett.* **1995**, *75*, 4472−4475.
(39) Hubbard, A. T., *Chem. Rev.* **1988**, *88*, 633−656.
(40) Goetting, L. B.; Huang, B. M.; Lister, T. E.; Stickney, J. L. *Electrochim. Acta* **1995**, *40*, 143−158.
(41) Kim, Y.-G.; Baricuatro, J. H.; Soriaga, M. P.; Suggs, D. W. *J. Electroanal. Chem.* **2001**, *509*, 170−174.

(42) Bravo, B. G.; Michelhaugh, S. L.; Soriaga, M. P.; Villegas, I.; Suggs, D. W.; Stickney, J. L. *J. Phys. Chem.* **1991**, *95*, 5245−5249.
(43) Brankovic, S. R.; Wang, J. X.; Adzic, R. R. *J. Serb. Chem. Soc.* **2001**, *66*, 887−898.
(44) Felter, T. E.; Hubbard, A. T. *J. Electroanal. Chem.* **1979**, *100*, 473−491.
(45) Inukai, J.; Osawa, Y.; Wakisaka, M.; Sashikata, K.; Kim, Y. G.; Itaya, K. *J. Phys. Chem. B* **1998**, *102*, 3498−3505.
(46) Martinez-Ruiz, A.; Valenzuela-Benavides, J.; de la Garza, L. M.; Batina, N. *Surf. Sci.* **2001**, *476*, 139−151.
(47) Stickney, J. L.; Villegas, I.; Ehlers, C. B. *J. Am. Chem. Soc.* **1989**, *111*, 6473−6474.